J. Comput. Phys. 494 (2023) 112534

Contents lists available at ScienceDirect

Journal of Computational Physics

journal homepage: www.elsevier.com/locate/jcp

Total of time variation diminishing principle for conservation laws

Gabor Toth

University of Michigan, 2455 Hayward St, Ann Arbor, MI, 48109, USA

ARTICLE INFO

Keywords:
Finite volume method
TVD
Stability
Conservation laws

ABSTRACT

We introduce a new principle for devising numerical schemes for conservation laws in one and multiple dimensions. The new formulation is based on the Total of Time Variation (TOTV) defined as the volume integral of the magnitude of the time derivative. For the one-dimensional scalar advection equation with a constant velocity, TOTV and the usual total variation (TV) are the same except for a constant factor. For non-linear equations and/or in multiple dimensions, TV and TOTV are different. We show that TOTV is a conserved quantity for one- and multi-dimensional scalar conservation laws with a non-linear flux function that can depend on the spatial coordinates as well. We call a numerical scheme that ensures that the discrete form of TOTV is not increasing in time a Total of Time Variation Diminishing (TOTVD) method. A TOTVD scheme is stable against catastrophic instabilities that would lead to uncontrolled growth of the time derivative. We show that the first order upwind scheme with a finite time step satisfying the usual CFL condition is TOTVD for all equations that satisfy the TOTVD property analytically. We demonstrate the difference between TV and TOTV with numerical tests.

1. Introduction

A large part of computational physics is concerned with solving systems of equations that can be written as conservation laws. For each conserved quantity u the time evolution is governed by

$$\partial_t u + \nabla \cdot \mathbf{f}_u(U, \mathbf{x}, t) = 0 \tag{1}$$

where $\mathbf{f}_u$ is a flux vector depending on the vector of conserved variables U, the coordinates $\mathbf{x}$ and time t in general. For sake of clarity, we use upper case for vectors and matrices of variables and bold face for vectors in the spatial coordinates. The conservation form of (1) ensures that the volume integral of u will only change due to the fluxes through the external boundaries.

Devising a scheme that can solve conservation laws accurately while maintaining stability and avoiding spurious oscillations is highly desirable. On the other hand, proving that a scheme will have these properties for the most general form of (1) is a daunting task. In practice, practitioners design schemes that have (some of) the desired properties for a subset of the equations and then hope that they will perform satisfactorily for a wider class of equations in practice.

One of the most successful class of numerical schemes solving (1) are based on the total variation diminishing (TVD) principle [1]. For a spatially one-dimensional case the total variation (TV) is defined as

$$T_x = \int dx |\partial_x u| \tag{2}$$

E-mail address: gtoth@umich.edu.

https://doi.org/10.1016/j.jcp.2023.112534
Received 25 May 2023; Received in revised form 20 September 2023; Accepted 28 September 2023

Available online 4 October 2023

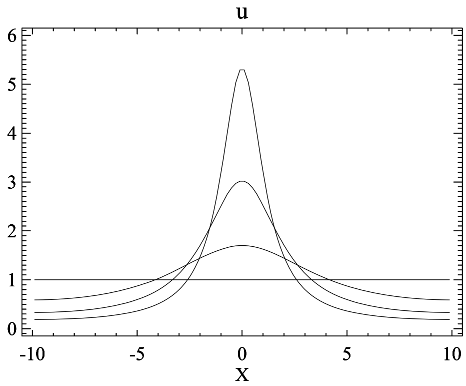

Fig. 1. Solution of a 1D scalar linear equation $\partial_t u - \partial_x(u \sin kx) = 0$ with initial condition $u = 1$. The four lines show the solutions at $t = 0, 1.69, 3.52$ and 5.34, respectively.

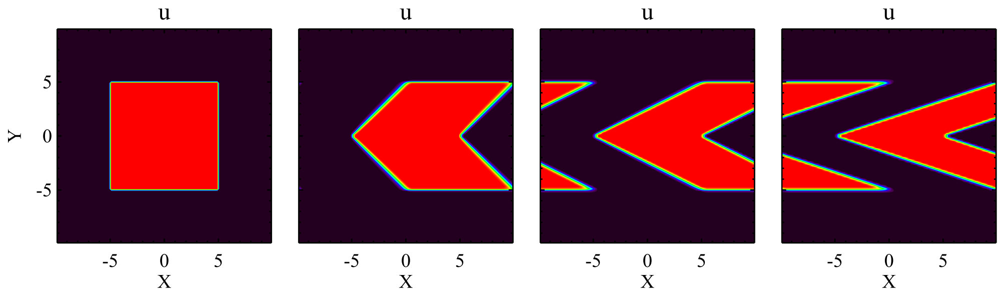

Fig. 2. Solution of the MD scalar equation $\partial_t u + \partial_x(u|y|) = 0$ on a double periodic 2D domain. The initial condition is $u = 1$ inside a square and 0 outside. The four plots show the solutions at $t = 0, 1, 2$ and 3 from left to right.

and the TVD property states that

$$T_x(t_2) \le T_x(t_1) \qquad \text{for} \quad t_2 > t_1 \tag{3}$$

The x subscript refers to the fact that T_x involves the x derivative. It can be shown that the analytic solution of a subset of (1) satisfies (3). For example, a scalar equation with flux $f = f(u)$ satisfies the TVD property, even if f is a non-linear function of u. Another example is the linear advection equation with $f = au$

$$\partial_t u + \partial_x(au) = 0, \tag{4}$$

where the velocity a is a constant. However, if a is a function of x, the TVD property does not hold. For example, if $a = \sin x$ and $u = 1$ initially at $t = 0$ then $T_x(0) = 0$. After a short time $t > 0$, the solution will have a wave like solution with a finite amplitude since $\partial_t u(x, 0) = -\partial_x(u \sin x) = -\cos x$ and $T_x(t) > T_x(0) = 0$ violates the TVD property (see Fig. 1).

Another important subset of the general conservation laws for which the TVD property is satisfied, is a system of linear (in U) hyperbolic equations with flux functions $F = \bar{A} \cdot U$, where $\bar{A}$ is a constant matrix with real eigenvalues. Such equations can be rewritten into scalar advection equations (4) for the characteristic variables W replacing U and the characteristic velocity λ_w replacing a. Then each of these equations satisfy the TVD property for each characteristic variable w.

Finally, for multi-dimensional (MD) scalar equations with $\mathbf{f} = \mathbf{f}(u)$, the MD TV defined as

$$T_\mathbf{x} = \int_V dV |\nabla u| \tag{5}$$

satisfies the MD TVD condition:

$$T_\mathbf{x}(t_2) \le T_\mathbf{x}(t_1) \qquad \text{for} \quad t_2 > t_1 \tag{6}$$

where $\mathbf{x}$ refers to the gradient with respect $\mathbf{x}$. While this is mathematically interesting, there are very few equations of interest that belong to this subset. The non-linear 2D Burgers equation with $\mathbf{f} = (u^2/2, u^2/2)$ and the MD linear advection equation with $\mathbf{f} = \mathbf{a}u$ (where $\mathbf{a}$ is a constant velocity vector) are two examples.

It is equally important to recognize that most of the equations of interest do not satisfy the TVD property. Important examples are non-linear systems of equations, such as the Euler equations in one or more dimensions. Another example is the advection of some scalar quantity in an arbitrary flow field with $\mathbf{f} = \mathbf{a}(\mathbf{x})u$, where the velocity vector $\mathbf{a}(\mathbf{x})$ depends on the coordinates (see Fig. 2 as an illustration). For the special case of divergence free flow field when $\nabla \cdot \mathbf{a} = 0$ and $0 = \partial_t u + \nabla \cdot (\mathbf{a}u) = \partial_t u + \mathbf{a} \cdot \nabla u =: Du/Dt$, Sokolov et al. [2] showed that the exact solution satisfies the TVD property for the TV defined as

$$T_s = \int_V dV \, |\nabla \cdot [\mathbf{a}(\mathbf{x})u]\,| = \int_V dV \, |\mathbf{a}(\mathbf{x}) \cdot \nabla u| \tag{7}$$

The interpretation of this functional in [2] is that T_s evaluates the spatial variation of u along streamlines. But there is an alternative and much more general interpretation based on the fact that $\nabla \cdot [\mathbf{a}(\mathbf{x})u] = \nabla \cdot \mathbf{f} = -\partial_t u$: in fact T_s is the volume integral of $|\partial_t u|$.

Based on this observation, we introduce the *total of time variation* (TOTV) as

$$T_t = \int_V dV \, |\partial_t u| \tag{8}$$

We will show that a surprisingly wide class of conservation laws satisfy the total of time variation diminishing (TOTVD) property

$$T_t(t_2) \le T_t(t_1) \qquad \text{for} \quad t_2 > t_1 \tag{9}$$

The TV and TOTV are related to each other in several ways. For differentiable functions $u(\mathbf{x}, t)$, one can define a space-time variation

$$T_{\mathbf{x},t} = \int_0^T dt \int_V dV (|\nabla u| + |\partial_t u|) = \int_0^T dt (T_{\mathbf{x}} + T_t) \tag{10}$$

that plays a central role in the theory of scalar conservation laws [3, chapter 2]. While the TVD property guarantees that $T_{\mathbf{x},t}$ is bounded, the TOTVD property does not in more than 1 spatial dimensions. This shows that the TOTVD property is less restrictive than the TVD property (6) defined for the MD case, because TOTVD restricts only 1 derivative with respect to time, while TVD restricts multiple derivatives with respect to space. This is not necessarily a disadvantage. There is an important subset of conservation laws that satisfy the TOTVD property but not the TVD property. In addition, the MD TVD property (6) is incompatible with second order accuracy [4]. In contrast, as demonstrated in [2], the TOTVD property can be enforced without breaking the global second-order of accuracy for the multi-dimensional advection equation with a spatially dependent divergence free velocity field. It is likely that second order TOTVD schemes exist for the more general MD scalar non-linear conservation laws with spatially dependent fluxes, although this is not proved or demonstrated in the present work.

The paper is structured as follows. Section 2 identifies the type of conservation laws that satisfy the TOTVD property. Section 3 establishes the numerical properties of TOTVD schemes. We prove that the first order upwind scheme has the TOTVD property as long as it satisfies the usual CFL condition in Section 4. In section 5 we perform numerical tests and compare the TOTVD scheme with the typical ad hoc multi-dimensional "TVD" schemes based on 1D TVD limiters. We conclude with section 6.

2. TOTVD conservation laws

In this section we identify some subsets of conservation laws (1) that satisfy the TOTVD property. We also contrast the TOTVD and TVD properties. For all equations we assume either periodic boundaries or zero flux through the boundary so that the global conservation of the conservative variable(s) is exact.

2.1. Linear scalar advection equation in 1D

We start with the simplest equation

$$\partial_t u + a\partial_x u = 0 \tag{11}$$

where $a \neq 0$ is the constant velocity. For this simple equation TOTV and TV are related as

$$T_t = |a| T_x \tag{12}$$

so the TVD and TOTVD conditions are analytically equivalent.

2.2. Multi-dimensional scalar conservation law

A MD conservation law for a scalar u can be written as

$$\partial_t u + \nabla \cdot \mathbf{f}(u, \mathbf{x}) = 0 \tag{13}$$

where the only restriction is that $\mathbf{f}$ does not depend explicitly on time. This will be needed, because we will use the time derivative of (13) in the proof. Before proceeding, we note again that (13) does not satisfy the TVD condition (6) in general, because the flux function depends explicitly on the coordinates.

The TOTV for u can be written as

$$T_t = \int_V dV|\partial_t u| = \int_V dV|\nabla\cdot\mathbf{f}(u,\mathbf{x})| \tag{14}$$

Let us split the computational domain V into two parts: in V^+ the time derivative $\partial_t u$ is positive or zero and in V^- it is negative. For continuous functions, $\partial_t u = 0$ must hold at the interfaces $\partial V^\pm$ between V^+ and V^-. The TOTV can be written as a sum of two integrals T_t^+ and T_t^- over V^+ and V^-, respectively:

$$T_t = T_t^+ + T_t^- \quad \text{where} \quad T_t^\pm = \pm\int_{V^\pm} dV\,\dot{u} \tag{15}$$

and $\dot{u} = \partial_t u$. The global conservation of u means that $T_t^+ - T_t^- = \int_V \dot{u} = 0$, so in fact

$$T_t = 2T_t^+ = 2T_t^- \tag{16}$$

so it is sufficient to show that T_t^+ is conserved. Notice that T_t^+ is the volume integral of $\dot{u}$ that satisfies the conservation law

$$\partial_t\dot{u} + \nabla\cdot\dot{\mathbf{f}}(u,\mathbf{x}) = 0 \tag{17}$$

which is the time derivative of the original conservation law (13). We can now apply the *Reynolds transport theorem* together with Gauss's divergence theorem to calculate the time derivative

$$\partial_t T_t^+ = \int_{\partial V^+} d\mathbf{S}\cdot\left(-\dot{\mathbf{f}}(u,\mathbf{x}) + \mathbf{v}_B(\mathbf{x})\dot{u}\right) \tag{18}$$

The first term on the right hand side is the integral of the flux $\dot{\mathbf{f}}$ over the surface of V^+, while the second term is the change due to the motion of the boundary with velocity $\mathbf{v}_B$. Note that only the normal (to the surface) component of $\mathbf{v}_B$ matters, which is uniquely defined. Since $\dot{u} = \partial_t u = 0$ at the surface, the second term vanishes. The first term can also be easily calculated from the chain rule:

$$\dot{\mathbf{f}}(u,\mathbf{x}) = \frac{\partial\mathbf{f}(u,\mathbf{x})}{\partial u}\frac{\partial u}{\partial t} = 0 \tag{19}$$

since, again, $\partial_t u = 0$ at the surface.

This completes our proof that the analytic solution of the scalar conservation law (13) conserves T_t and therefore it satisfies the TOTVD property (9). We note that the linear conservation laws with divergence-free velocity considered by [2] is a subset of the conservation laws described by (13). It is also important to note that the definition of TOTV (8) and the proof of the TOTVD property (9) are only valid for differentiable $u(\mathbf{x},t)$ functions. Generalization to discontinuous functions is left for future work.

2.3. Linear system of hyperbolic conservation laws in 1D

Here we consider a vector of unknowns U with N_U elements that satisfy the conservation law

$$\partial_t U + \partial_x(\bar{A}\cdot U) = 0 \tag{20}$$

where $\bar{A}$ is a constant $N_U \times N_U$ matrix with N_U real eigenvalues, and N_U left and N_U right eigenvectors that form an orthonormal basis. The characteristic variables can be defined as $W = \bar{L}\cdot U$, where $\bar{L}$ is a matrix formed from the left eigenvectors of $\bar{A}$. Conversely, U can be expressed as $U = \bar{R}\cdot W$ where $\bar{R} = \bar{L}^{-1}$ is the matrix of right eigenvectors. Substituting into (20) results in

$$\partial_t\bar{R}\cdot W + \partial_x(\bar{\Lambda}\cdot\bar{R}\cdot W) = 0 \tag{21}$$

where $\bar{\Lambda}$ is a diagonal matrix formed from the eigenvalues λ_w. Multiplying (21) with the left eigenvector matrix from the left results in

$$\partial_t W + \partial_x(\bar{\Lambda}\cdot W) = 0 \tag{22}$$

which is set of N_U independent linear advection equations that can be written as

$$\partial_t w + \nabla\cdot(\lambda_w w) = 0 \tag{23}$$

for each characteristic variable v. Since (23) is a linear 1D advection equation identical to (11), the TOTVD scheme coincides with the TVD scheme for each characteristic variable.

While the 1D linear system of equations does not seem very common in practical problems, the very successful TVD schemes applied to systems of equations in multiple dimensions are all based on the 1D linear system of equations. In essence, the TVD schemes are applied to a linearized form of the non-linear system of equations separately for each dimension. The resulting schemes are routinely and successfully used to solve the general conservation laws (1).

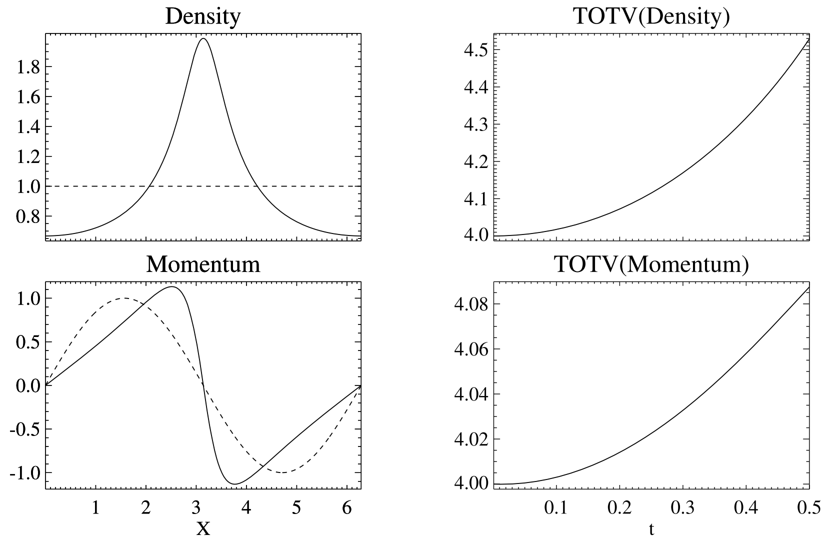

Fig. 3. Left: initial condition (dashed) and solution at $t = 0.5$ (solid) of the isothermal hydrodynamic problem. Right: time evolution of the TOTV of density and momentum.

Table 1
Subsets of conservation laws with no explicit time dependence.

Equation	Flux	TVD	TOTVD	Equivalent
Linear 1D scalar	au	Yes	Yes	Yes
Linear 1D scalar (x)	$a(x)u$	No	Yes	No
Linear MD scalar	$\mathbf{a}u$	Yes (1st order)	Yes	Yes
Linear MD scalar $(\mathbf{x})$	$\mathbf{a}(\mathbf{x})u$	No	Yes	No
Non-linear 1D scalar	$f(u)$	Yes	Yes	No
Non-linear 1D scalar (x)	$f(u,x)$	No	Yes	No
Non-linear MD scalar	$\mathbf{f}(u)$	Yes (1st order)	Yes	No
Non-linear MD scalar $(\mathbf{x})$	$\mathbf{f}(u,\mathbf{x})$	No	Yes	No
Linear 1D system	$\bar{A} \cdot U$	Yes	Yes	Yes
Non-linear 1D system	$F(U)$	No	No	–
Non-linear MD system	$\mathbf{F}(U)$	No	No	–

2.4. Nonlinear system

A simple example for a 1D non-linear system is the hydrodynamic equations for isothermal gas. The conservative variables $U = (\rho, m)$ are the mass and momentum densities. The fluxes are $F = (m, m^2/\rho + k\rho)$, where k is a constant related to temperature. Let us consider a 1D problem with initial condition $\rho = 1$, $m = \sin(x)$ and $k = 0.1$ on a periodic domain $[0, 2\pi]$. Fig. 3 shows the converged numerical solution (obtained on a grid of 5,000 cells with the first order upwind scheme) at $t = 0.5$ together with the time variation of $TOTV$ for both ρ and m (TV is increasing for both variables, and is not shown). Clearly, TOTV is monotonically increasing with time for both variables and it seems impossible to construct a combination of these quantities that would satisfy a TOTVD-like property. We conclude that a nonlinear system of equations is neither TVD, nor TOTVD in general.

2.5. Summary of TOTVD conservation laws

We summarize the findings of this section in Table 1. For the 1D linear equations the two principles are equivalent. For non-linear scalar equations both principles apply, but TVD contradicts second order of accuracy in the MD case. The TOTVD principle applies to all scalar conservation laws with coordinate dependent fluxes $\mathbf{f} = \mathbf{f}(u, \mathbf{x})$. Conversely, conservation laws with purely time dependent flux functions $\mathbf{f} = \mathbf{f}(u, t)$ are TVD, but not TOTVD. The spatially variable flux involves a much richer set of equations than the time dependent flux, simply because there is only one time variable but there can be multiple spatial coordinates in MD. The MD scalar equations with coordinate dependent fluxes are practically important, and for these equations only the TOTVD concept applies. Non-linear systems are neither TVD nor TOTVD in general.

2.6. 1D example

Finally, we demonstrate how significant the difference can be between TV and TOTV. Fig. 1 shows the solution of

$$\partial_t u + \partial_x(-u \sin kx) = 0, \qquad k = \frac{2\pi}{20} \tag{24}$$

on the $[-10, 10]$ domain with periodic boundary conditions. The initial condition is $u(x,0) = 1$. The 4 curves show the solution at $t = 0, 1.69, 3.52$ and 5.34. The peak at $x = 0$ grows exponentially, because at $x = 0$ the equation reduces to

$$\partial_t u = ku \tag{25}$$

since $\cos 0 = 1$ and $\partial_x u(0,t) = 0$. The TV therefore goes to infinity, on the other hand the TOTV is finite ($T_t = 20$), it is conserved analytically, and it diminishes numerically.

2.7. MD example

The 1D example had locally growing solution due to the non-zero divergence of the "velocity" $v = \partial_u f = -\sin kx$. But TV can grow even if the maximum of the solution does not. Let us consider a 2D equation

$$\partial_t u + \partial_x(u|y|) = 0 \tag{26}$$

describing a shear flow on a double periodic domain $-10 < x, y < 10$. The velocity field $\mathbf{a} = \mathbf{f}/u = (|y|, 0)$ has zero divergence. The initial condition is $u(x,y,0) = 2$ inside a square $-5 < x, y < 5$ and $u(x,y,0) = 1$ outside. Fig. 2 demonstrates the time evolution. The shear will distort the square increasing its TV roughly linearly with time $T_\mathbf{x} \to \infty$ as $t \to \infty$. In contrast, the TOTV remains constant.

3. Properties of TOTVD schemes

In this subsection we prove that a TOTVD scheme is stable against catastrophic instabilities and show that it does not directly suppress spurious spatial oscillations.

First of all, we need to discretize (8). A very natural discretization is

$$T^n = \sum_i V_i \frac{|\Delta_n u_i|}{\Delta_n t} \tag{27}$$

where u_i^n is the cell average value in cell i at time step n. The Δ_n operator takes the difference between time steps $n+1$ and n, or formally for any quantity q:

$$\Delta_n q := q^{n+1} - q^n \tag{28}$$

The symbol Δ without a subscript will be used as a short hand notation for Δ_n when n is known from the context. V_i is the volume of cell i, and t_n is the time at step n. For the sake of simplicity, we assume that the temporal update consists of a single stage. We will consider multi-stage TOTVD schemes at the end of this section.

3.1. Stability

It is clear that the TOTV defined by (8) is intimately related to stability. Numerical instabilities typically manifest themselves in an exponential growth of the amplitude of the solution, which means that the magnitude of the time derivative $|\partial_t u|$ will also grow exponentially, so that the TOTV will grow unbounded as well.

To make this argument more formal, let us assume that the maximum magnitude of the solution defined as $M^n = \max_i |u_i^n|$ grows faster than linear starting from time step m:

$$M^n > M^m + c(t_n - t_m)^\alpha \qquad \text{for} \quad n > m \tag{29}$$

where $c > 0$ and $\alpha > 1$ are constants. The magnitude of the largest discrete time derivative is then bounded as

$$\max_{k\in[m,n-1],i} \frac{|\Delta_k u_i|}{\Delta_k t} \ge \max_{k\in[m,n-1]} \frac{M^{k+1} - M^k}{t_{k+1} - t_k} \ge \frac{M^n - M^m}{t_n - t_m} > c(t_n - t_m)^{\alpha-1} \tag{30}$$

which grows unbounded as $t_n \to \infty$. This means that the maximum of the discrete TOTV, which is a sum of positive contributions from the grid cells including the cell with the maximum change,

$$\max_{k\in[m,n-1]} T^k = \max_{k\in[m,n-1]} \sum_i \frac{|\Delta_k u_i|}{\Delta_k t} \ge \max_{k\in[m,n-1],i} \frac{|\Delta_k u_i|}{\Delta_k t} > c(t_n - t_m)^{\alpha-1} \tag{31}$$

will also grow unbounded.

The solution of $\partial_t u = \partial_x(u \sin kx)$ has a maximum value at $x = 0$ that goes to infinity exponentially with time, $u(0,t) = u(0,0)\exp(kt)$, still the TOTV is conserved (see subsection 2.6). This may seem to contradict the proof above, but it does not. In the proof we

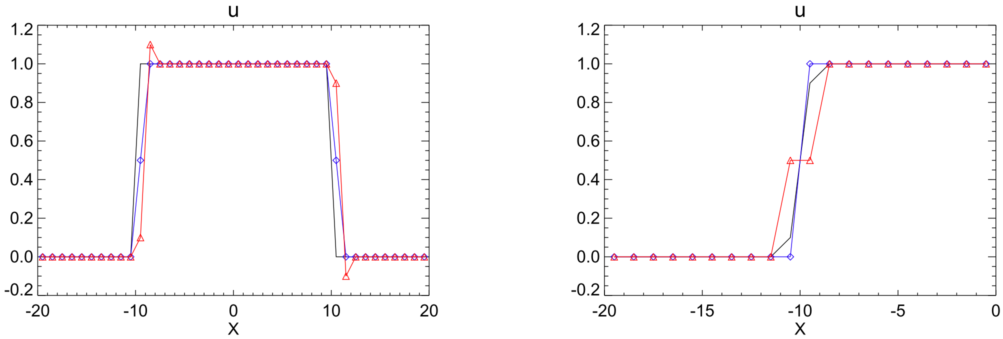

Fig. 4. Left: hypothetical numerical solution for the advection equation $\partial_t u + \partial_x u = 0$ on a uniform grid with $\Delta x = 1$. The initial condition is a square wave (black line). The numerical solution at $t = 0.5$ and $t = 1$ are shown with blue diamonds and red triangles, respectively. The TV increased from $t = 0.5$ to $t = 1$, but the TOTV remained the same despite the overshoot at $x = -10.5$ and undershoot at $x = 11.5$. Right: hypothetical numerical solution for a stationary (or slowly moving) sharp profile. The initial condition is shown by the black line. In the first time step it sharpens into a pure jump (blue diamonds), and in the second time step creates a staircase function (red triangles). All these changes satisfy the conservation law and the TVD property, but they violate TOTVD, as the magnitude of the time derivative is increasing. (For interpretation of the colors in the figure(s), the reader is referred to the web version of this article.)

assumed that there is a finite size grid cell with a discrete value whose magnitude grows faster than linear. The solution is positive everywhere and the volume integral of u is conserved both analytically and numerically (we took periodic boundaries), so the cell with the maximum value cannot exceed the sum of the initial cell values $S^0 = \sum_i u_i^0$. This means that while the analytic maximum value $u(0,t) \to \infty$ exponentially, the discrete maximum value M^n is bounded from above by S. Conversely, one could wonder if the conservation property excludes the unlimited growth of a cell value, which would render the proof about stability meaningless. Fortunately, that is not the case either. For a conservative scheme the typical numerical instability manifests as a short wavelength oscillation with exponentially increasing magnitude. The cell values will have opposite signs, so the sum S^n will be conserved, but the maximum magnitude M^n increases exponentially.

We proved that a scheme satisfying (27) cannot be unstable with a growth rate exceeding linear growth, so in practice this means that a TOTVD scheme is stable.

3.2. Spurious oscillations

The TVD condition guarantees that the solution remains oscillation free. This is easiest to see for the 1D scalar equation

$$\partial_t u + \partial_x f(u) = 0 \tag{32}$$

The TV defined in (3) is equal to the differences of local extrema:

$$T_x = \sum_{e=1}^{E-1} |u(x_e) - u(x_{e+1})| \tag{33}$$

where $x_1 < x_2 < \ldots < x_E$ are the locations of the local extrema including the values at non-periodic boundaries (for periodic boundaries there is an additional term $|u(x_E) - u(x_1))|$ in the sum). If any of the extrema become more extreme or any new extrema appear, while other extrema do not change, T_x will get larger. Since the extrema are separated from each other, changes at one local extremum have no causal relationship with changes at another one (unless they are in neighboring cells). This means that the global TVD property is sufficient to guarantee that there will be no new extrema.

The TOTVD property, by itself, does not guarantee that no spurious oscillations appear, because it constrains the temporal change rather than the spatial gradients. To demonstrate this, let us consider the propagation of a square wave in 1D. The advection equation with velocity $a = 1$ is

$$\partial_t u + \partial_x u = 0 \tag{34}$$

and the initial condition is $u(x,0) = 1$ for $|x| < 10$ and 0 otherwise on a periodic domain of $-20 \le x \le 20$. Let us use a uniform grid consisting of 40 cells of size $\Delta x = 1$, so initially $u_i^0 = 1$ for $i = 11 \ldots 30$ and 0 in the rest of the cells. We will fix the time step to $\Delta t = 0.5$. The analytic as well as the discrete TV is $T_x = 2$ due to the two jumps at $x = \pm 10$.

Assuming that the scheme is exact in the finite volume sense with this initial data, the solution in the first time step changes only in cells 11 and 31: from $u_{11}^0 = 1$ to $u_{11}^1 = 0.5$ and from $u_{31}^0 = 0$ to $u_{31}^1 = 0.5$, so the discrete TOTV is $T_t^0 = (0.5 + 0.5)/\Delta t = 2$. Let us assume that in the next time step the solution changes from $u_{11}^1 = 0.5$ to $u_{11}^2 = 0.1$, from $u_{12}^1 = 1$ to $u_{12}^2 = 1.1$, from $u_{31}^1 = 0.5$ to $u_{31}^2 = 0.9$ and from $u_{32}^1 = 0$ to $u_{32}^2 = -0.1$ due to some overly zealous anti-diffusive scheme that is trying to sharpen the solution. The changes are conservative, $\sum_i u_i^n = 20$ for $n = 0, 1, 2$, but new extrema were created in cells 12 and 32. The TV has increased from 2 to 2.2, but the TOTV did not change, since $T_t^1 = (0.4 + 0.1 + 0.4 + 0.1)/\Delta t = 2 = T_t^0$. Fig. 4 shows this hypothetical numerical solution.

It is noteworthy that the analytic TV and TOTV are equivalent for this equation according to (12), but the discrete TV and TOTV are different in general, since TV is the sum of differences of neighboring cell values $|u_i - u_{i-1}|$, while TOTV is the sum of differences of neighboring cell interface fluxes $|f_{i+1/2} - f_{i-1/2}|$. The truncation errors of the discretization can break the analytic proportionality $f = au$, which results in different consequences for the TVD and TOTVD schemes.

For 1 spatial and 1 temporal dimension, the TVD and TOTVD conditions are, in some sense, symmetric: TVD restricts oscillations in space, while TOTVD restricts oscillations in time. The right panel of Fig. 4 shows a hypothetical temporal oscillation that would be allowed by a TVD scheme, but not by TOTVD. The amplitude of the spatial/temporal oscillations is limited by the neighboring extrema in the spatial/temporal variation. One major difference, however, is that TVD prohibits development of new extrema in u, while TOTVD does not. This property of TVD is important for ensuring positivity, for example.

While the TOTVD property does not prohibit spurious spatial oscillations, it does not mean that a TOTVD scheme will necessarily produce them (similarly, a TVD scheme will not necessarily produce temporal oscillations). Properly used upwind fluxes and TVD-based limiters can suppress spatial oscillations successfully even for equations that do not satisfy the TVD condition. The TOTVD property can be used as an additional constraint to guarantee stability and further reduce the chances of producing ill-behaved numerical solutions.

4. TOTVD schemes

A single stage finite volume scheme solving the scalar conservation law (13) can be written as

$$\frac{\Delta u_i}{\Delta t} = -\frac{1}{V_i}\sum_s \mathbf{A}_{s,i}\cdot \mathbf{f}^n_{s,i} = -\frac{1}{V_i}\sum_s \varphi^n_{s,i} \tag{35}$$

The s index refers to the faces of cell i with volume V_i and outward pointing face vectors $\mathbf{A}_{s,i}$. The face centered flux vector is $\mathbf{f}^n_{s,i}$, and $\varphi^n_{s,i} := \mathbf{A}_{s,i}\cdot\mathbf{f}^n_{s,i}$ is the normal flux through the cell face. While using abstract notation for cell centers and cell faces is common, it is possible to make the notation precise. For a 3D Cartesian grid with $N\times N\times N$ grid cells, the index $i = 1,\ldots,N^3$ lists cells in a natural order of sweeping through the first dimension first, then the second, and finally the third. The neighbors of cell i are $i\pm 1$, $i\pm N$ and $i\pm N^2$ assuming that cell i is not near any boundary. To make it easy to refer to these neighbor cells, the sides are indexed with $s\in S = \{\pm 1, \pm N, \pm N^2\}$ instead of the usual $1,\ldots,6$. The s face of cell i will be denoted as subscript s,i. This notation allows for expressing spatial relationships in a precise form. For example, the s,i face coincides with the $-s,i+s$ face, while the opposite $-s,i$ face coincides with the $s,i-s$ face. A conservative discretization requires

$$\varphi^n_{s,i} = -\varphi^n_{-s,i+s} \tag{36}$$

The TOTV defined in (27) can be written as

$$T^n = \sum_i \left|\sum_s \varphi^n_{s,i}\right| \tag{37}$$

where we dropped the t subscript for simplicity. Similar to the analytic case (15), we can split the computational grid into two sets of cells I^n_+ and I^n_-, where the solution is increasing ($\partial_t u_i \ge 0$ for $i\in I^n_+$) and decreasing ($\partial_t u < 0$ for $i \in I^n_-$), respectively:

$$T^n = T^n_+ + T^n_- \qquad T^n_\pm = \mp\sum_{I^n_\pm}\sum_s \varphi^n_{s,i} \tag{38}$$

Similar to the analytic case (16), the two partial sums are equal due to the global conservation of $\sum_i (V_i u_i)$ and

$$T^n = 2T^n_+ = 2T^n_- \tag{39}$$

The summation in (38) reduces to the cell faces at the boundaries of the $I^n_\pm$ sets since the internal fluxes cancel out. The sets of boundary faces $B^n_\pm$ are defined as follows: for $(i,s)\in B^n_+$, $i\in I^n_+$ and $(i{+}s)\in I^n_-$, while for $(i,s)\in B^n_-$, $i\in I^n_-$ and $(i{+}s)\in I^n_+$. We note that the two sets are different, but in fact they refer to the same cell faces, just relating them to different cell centers. With this definition we have

$$T^n_\pm = \mp\sum_{B^n_\pm}\varphi^n_{s,i} \tag{40}$$

4.1. Necessary condition

First we consider a small time step when the boundaries of the $I^n_\pm$ sets do not change, and the discrete change of $T^n = 2T^n_\pm$ is proportional to the sum of the time derivatives of $\varphi_{s,i}$ along the boundary. To simplify the notation, we will drop the n superscripts in this subsection. Taking the time derivative of (40), the scheme is TOTVD if

$$\dot{T}_\pm = \mp\sum_{B_\pm}\dot{\varphi}_{s,i} \le 0 \tag{41}$$

To proceed, we need to define the discrete face flux function. There are several possibilities, but for sake of simplicity, we assume that the face flux is calculated from the face state $u_{s,i}$ obtained from a linear combination of nearby cell center values:

$$u_{s,i} = \sum_d \alpha_{d,s,i} u_{i+ds} \tag{42}$$

$$\varphi_{s,i} = \mathbf{A}_{s,i} \cdot \mathbf{f}(u_{s,i}, \mathbf{x}_{s,i}) \tag{43}$$

where the coefficients $\alpha_{d,s,i}$ will be determined later. The index d covers the stencil, for example $d = 0$ and $d = 1$ refer to the cell and its s neighbor, respectively. Consistency requires that $\sum_d \alpha_{d,s,i} = 1$. In addition, requiring $\alpha_{d,s,i} \geq 0$ helps preserving positivity and avoiding oscillations. A simple second order accurate interpolation has $\alpha_{0,s,i} = \alpha_{1,s,i} = 1/2$ taking the arithmetic average of the cell center values on the two sides of face s.

We can now substitute the discrete normal flux from (43) into (41) and apply the chain rule

$$\dot{T}_\pm = \mp \sum_{B_\pm} \mathbf{A}_{s,i} \cdot \partial_u \mathbf{f}(u_{s,i}, \mathbf{x}_{s,i}) \dot{u}_{s,i} = \mp \sum_{B_\pm} a_{s,i}(u_{s,i}) \sum_d \alpha_{d,s,i} \dot{u}_{i+ds} \tag{44}$$

where we introduced the “normal velocity”

$$a_{s,i}(u) := \mathbf{A}_{s,i} \cdot \mathbf{v}(u, \mathbf{x}_{s,i}) \tag{45}$$

and the “velocity”

$$\mathbf{v}(u, \mathbf{x}) := \partial_u \mathbf{f}(u, \mathbf{x}) \tag{46}$$

When $a_{s,i}(u_{s,i}) > 0$, the velocity points outward from cell i towards cell $i+s$, when $a_{s,i}(u_{s,i}) < 0$, the velocity vector points towards cell i.

Let us consider $\dot{T}_+$ that is expressed as a sum over faces B_+, so $i \in I_+$ and $\dot{u}_i \geq 0$, while $i+s \in I_-$ and $\dot{u}_{i+s} < 0$. From (44), the time derivative of T_+ will be non-positive if

$$-a_{s,i}(u_{s,i}) \sum_d \alpha_{d,s,i} \dot{u}_{i+ds} \leq 0 \tag{47}$$

for every cell face in B_+. A simple choice for $\alpha_{d,s,i}$ that guarantees $\dot{T}_+ \leq 0$ is

$$\begin{aligned} \beta_{s,i} &:= \alpha_{0,s,i} = 1; \quad u_{s,i} = u_i \quad &&\text{for} \quad a_{s,i}(u_{s,i}) \geq 0, \\ \gamma_{s,i} &:= \alpha_{1,s,i} = 1; \quad u_{s,i} = u_{i+s} \quad &&\text{for} \quad a_{s,i}(u_{s,i}) < 0, \end{aligned} \tag{48}$$

which is *the first order upwind scheme*. The upwind direction is determined by the velocity $\mathbf{v}$: when it points outward from cell i, the cell center state u_i is used, when it points inward, the neighbor cell state u_{i+s} is used to calculate the flux. We introduced $\beta_{s,i}$ and $\gamma_{s,i}$, the weight of the cell and the neighbor cell, respectively, to simplify the notation.

There is a circular dependency in (42), (45) and (48), because the definition of $a_{s,i}$ depends on $\alpha_{d,s,i}$, and vice versa. To resolve this, we define the upwind direction based on the cell center states instead of the state at the face:

$$\begin{aligned} u_{s,i} &= u_i \quad &&\text{if} \quad a_{s,i}(u_i) + a_{s,i}(u_{i+s}) \geq 0 \\ u_{s,i} &= u_{i+s} \quad &&\text{if} \quad a_{s,i}(u_i) + a_{s,i}(u_{i+s}) < 0 \end{aligned} \tag{49}$$

For typical cases the two cell center based velocities $a_{s,i}(u_i)$ and $a_{s,i}(u_{i+s})$ have the same signs that also agrees with the sign of the face value based velocity $a_{s,i}(u_{s,i})$.

We proved that the first order upwind flux satisfies the TOTVD property $T^{n+1} \leq T^n$ where T^n is defined by (27) as long as the sets of cells with increasing and decreasing values do not change.

4.2. First order upwind scheme is TOTVD

For an arbitrary time step, the TOTVD condition for $T_+ = T/2$, based on (38), can be written as

$$-\Delta T_+ = \sum_{I_+^{n+1}, s} \varphi_{s,i}^{n+1} - \sum_{I_+^n, s} \varphi_{s,i}^n \geq 0 \tag{50}$$

We can split the set I_+^{n+1} into two disjoint subsets: $I_+^+ = I_+^n \cap I_+^{n+1}$ for the cells that were and keep increasing and $I_-^+ := I_-^n \cap I_+^{n+1}$ for the newly added I_+ cells. Similarly, I_+^n can be split into I_+^+ and $I_+^- = I_+^n \cap I_-^{n+1}$, the cells that no longer grow in time step $n+1$. Using these subsets the condition becomes:

$$\sum_{I_+^+, s} (\varphi_{s,i}^n + \Delta\varphi_{s,i}) + \sum_{I_-^+, s} (\varphi_{s,i}^n + \Delta\varphi_{s,i}) - \sum_{I_+^+, s} \varphi_{s,i}^n - \sum_{I_+^-, s} \varphi_{s,i}^n \geq 0 \tag{51}$$

Grouping terms with superscripts n and with changes Δ separately gives

$$\sum_{I_+^+, s} \Delta\varphi_{s,i} + \sum_{I_-^+, s} \Delta\varphi_{s,i} + \sum_{I_-^+, s} \varphi_{s,i}^n - \sum_{I_+^-, s} \varphi_{s,i}^n \geq 0 \tag{52}$$

Finally we can cancel out internal normal fluxes in the first two sums, and sum over the boundary faces only:

$$\sum_{B_+^+} \Delta\varphi_{s,i} + \sum_{B_-^+} \Delta\varphi_{s,i} + \sum_{I_-^+,s} \varphi_{s,i}^n - \sum_{I_+^-,s} \varphi_{s,i}^n \geq 0 \tag{53}$$

where B_+^+ and B_-^+ are the boundary faces surrounding I_+^+ and I_-^+, respectively. This inequality is the discretized form of (18). There are three possible reasons for the left side to be different from 0:

1. The normal flux $\varphi_{s,i}$ changes at the boundary B_+^+ and B_-^+ (first two sums).
2. Cells at the edge of I_+^n become part of I_-^{n+1} or vice versa (last two sums).
3. Cells in the middle of I_+^n become part of I_-^{n+1} or vice versa (last two sums).

The first one is the discrete equivalent of (41). The second reason is the discrete motion of the boundary corresponding to the second term in (18). The third reason corresponds to a spurious oscillation in the time derivative, which should be avoided.

4.2.1. Proof of TOTVD for the first order upwind scheme with finite time step

We will prove that the first order upwind scheme guarantees that changes due to the first and second causes are non-negative, and the third does not happen as long as the time step obeys an appropriate CFL condition.

In the first two sums in (53) we can write the change in the normal fluxes as

$$\Delta\varphi_{s,i} = \mathbf{A}_{s,i} \cdot \partial_u \mathbf{f}(u_{s,i}^*, \mathbf{x}_{s,i})\Delta u_{s,i} = a_{s,i}(u_{s,i}^*)\Delta u_{s,i} \tag{54}$$

where $u_{s,i}^* \in [u_{s,i}^n, u_{s,i}^{n+1}]$ is some intermediate value between the two time steps. The existence of u^* is guaranteed by the differentiability of the flux function $\mathbf{f}(u, \mathbf{x})$ and the mean value theorem. For a well-behaved flux function, we expect $a_{s,i}(u_{s,i}^*) \in [a_{s,i}(u_i), a_{s,i}(u_{i+s})]$. To further simplify the expressions, we use the shorthand notation $a_{s,i}^* := a_{s,i}(u_{s,i}^*)$. Note that for a linear flux function $a_{s,i}$ does not depend on u. In the last two sums in (53), $\sum_s \varphi_{s,i}^n$ can be replaced with $-(V_i/\Delta t)\Delta u_i$. With these changes (53) becomes:

$$\sum_{B_+^+} a_{s,i}^*\Delta u_{s,i} + \sum_{B_-^+} a_{s,i}^*\Delta u_{s,i} - \sum_{I_-^+} \frac{V_i}{\Delta t}\Delta u_i + \sum_{I_+^-} \frac{V_i}{\Delta t}\Delta u_i \geq 0 \tag{55}$$

In the third sum $\Delta u_i \leq 0$ since $i \in I_-^+ \subset I_-^n$. In the fourth sum $\Delta u_i \geq 0$ as it is over cells in $I_+^- \subset I_+^n$. In both cases, we can replace Δt with a larger or equal value based on the CFL condition and the left hand side will not increase. We now assume, and then later prove, that the CFL condition can be written as

$$\Delta t \leq C \frac{V_i}{\sum_s a_{s,i}^+} \tag{56}$$

where $a_{s,i}^+ := \max(0, a_{s,i}^*)$ and $C \leq 1$ is the CFL coefficient. Using the CFL condition to replace Δt a sufficient inequality for (55) is

$$\sum_{B_+^+} a_{s,i}^*\Delta u_{s,i} + \sum_{B_-^+} a_{s,i}^*\Delta u_{s,i} + \sum_{I_-^+,s} a_{s,i}^+|\Delta u_i| + \sum_{I_+^-,s} a_{s,i}^+|\Delta u_i| \geq 0 \tag{57}$$

In the third sum $\Delta u_i \leq 0$ was replaced with $-|\Delta u_i|$ and in the last sum $\Delta u_i \geq 0$ was replaced with $|\Delta u_i|$ to make positivity arguments simpler. The last two sums contribute with all non-negative terms. In the third sum over I_-^+, s we can drop the positive contributions from faces that are not in B_-^+, so it can be combined with the second sum. Finally, for the upwind scheme $a_{s,i}^*\Delta u_{s,i} = a_{s,i}^+\Delta u_i + a_{s,i}^-\Delta u_{i+s}$ in the first two sums, where $a_{s,i}^- := \min(0, a_{s,i}^*)$. After applying these changes the sufficient condition is

$$\sum_{B_+^+} \left(a_{s,i}^+|\Delta u_i| + a_{s,i}^-\Delta u_{i+s} \right) + \sum_{B_-^+} a_{s,i}^-\Delta u_{i+s} + \sum_{I_+^-,s} a_{s,i}^+|\Delta u_i| \geq 0 \tag{58}$$

The only terms that can be negative are $a_{s,i}^-\Delta u_{i+s}$. This requires $\Delta u_{i+s} > 0$ so $(i+s) \in I_+^n$. On the other hand, in the first sum $(i+s) \notin I_+^+$, so $(i+s) \in I_+^-$. Using the $a_{s,i}^- = -a_{-s,i+s}^+$ identity, we can move this term into the last sum. In the second sum $\Delta u_{i+s} > 0$ requires that $(i+s) \in I_+^n = I_+^+ \cup I_+^-$. If $(i+s) \in I_+^+$, then the term can be moved into the first sum as its $-s$ neighbor $i \notin I_+^+$ so face $-s, i+s \in B_+^+$. If $(i+s) \in I_+^-$ then the term can be moved into the last sum. In the modified last sum a given face $(-s, i+s)$ either comes from the first or the second sum depending on the sign of Δu_i, so it can only occur at most once. By including all faces with negative contributions into the first and last sums, the left hand side reduces, and the following sufficient condition is obtained

$$\sum_{B_+^+} (a_{s,i}^+ - a_{s,i}^+)|\Delta u_i| + \sum_{I_+^-,s} (a_{s,i}^+ - a_{s,i}^+)|\Delta u_i| \geq 0 \tag{59}$$

The left hand side is identically zero, so the original inequality (53) holds.

We have proved that the first order upwind scheme with a finite time step satisfying the CFL condition (56) is TOTVD.

4.2.2. No negative change inside I_+ for first order upwind scheme

An additional desirable property, although not necessary for the TOTVD property, is that a cell inside I_+ does not become part of I_- in a single time step. The requirement is that

$$V_i \frac{\Delta_{n+1} u_i}{\Delta_{n+1} t} = -\sum_s (\varphi^n_{s,i} + \Delta\varphi_{s,i}) = V_i \frac{\Delta u_i}{\Delta t} - \sum_s a^*_{s,i} \Delta u_{s,i} \geq 0 \tag{60}$$

if cell $i \in I_+$ and all its neighbors $i+s \in I_+$, so $\Delta u_i \geq 0$ and $\Delta u_{i+s} \geq 0$ for all s indexes. The first term $V_i \Delta u_i / \Delta t$ can be estimated from the CFL condition (56). In the second term $\Delta u_{s,i} > 0$ from (49) if the signs of $a_{s,i}(u_i)$ and $a_{s,i}(u_{i+s})$ do not change from time step n to time step $n+1$. This means that in (60) terms with $a^*_{s,i} \leq 0$ coefficients increase the left hand side of the inequality, so they can be safely dropped by replacing $a^*_{s,i}$ with $a^+_{s,i} := \max(0, a^*_{s,i})$. For the other terms with $a^*_{s,i} > 0$, the first order upwind flux sets $\Delta u_{s,i} = \Delta u_i$, so a sufficient condition for inequality (60) is

$$\sum_s a^+_{s,i} \Delta u_i - \sum_s a^+_{s,i} \Delta u_i \geq 0 \tag{61}$$

which is obviously true. A similar proof can be employed to show that no cells belonging to I_+ pop up inside I_-.

We have proved that the first order upwind scheme satisfying the CFL condition does not produce new I_- cells inside I_+ or vice versa, which is the TOTVD analogue of the TVD schemes not creating spurious spatial oscillations.

4.2.3. Properties of the first order upwind scheme

Combining the previous results, we proved that the first order upwind flux with a time step limited by the CFL condition (56) satisfies the TOTVD property and does not generate spatial-temporal oscillations. While this result is similar to the well-known theorem that the first order upwind scheme is TVD, it is actually quite different. The first order upwind scheme applied to the example equations in subsections 2.6 and 2.7 will not produce TVD results, but they satisfy the TOTVD property. This proof is also more general than the result obtained for the linear divergence-free transport equation [2].

4.3. Second order TVD scheme

We will evaluate the TOTVD property, or lack of it, of the usual second order TVD schemes that apply the limiters on a dimension-by-dimension basis. For the monotonized central (MC) limiter the face value $u_{s,i}$ is constructed from the cell center values at $i-s, i$ and $i+s$ as

$$u_{s,i} = u_i + \frac{1}{2}\operatorname{minmod}\left(\beta(u_{i+s} - u_i), \frac{1}{2}(u_{i+s} - u_{i-s}), \beta(u_i - u_{i-s})\right) \tag{62}$$

when the velocity points from cell i to $i+s$. Otherwise the same formula is used but centered on cell $i+s$. The parameter β is in the range $[1,2]$. For $\beta = 1$ the MC limiter becomes the standard minmod limiter, since the middle term $(u_{i+s} - u_{i-s})/2$ in the minmod function can be removed in this case. In the numerical tests, we will imply $\beta = 2$ when we refer to the MC limiter and $\beta = 1$ for the minmod limiter.

For second order accuracy in time, the usual midpoint method is employed:

$$u_i^{n+1/2} = u_i^n - \frac{\Delta t}{2V_i} \sum_s \varphi^n_{s,i} \tag{63}$$

$$u_i^{n+1} = u_i^n - \frac{\Delta t}{V_i} \sum_s \varphi^{n+1/2}_{s,i} \tag{64}$$

The final update looks just like the one-stage scheme, except for using $u^{n+1/2}$ in the normal flux:

$$\varphi^{n+1/2}_{s,i} := \mathbf{A}_{s,i} \cdot \mathbf{f}(u^{n+1/2}_{s,i}, \mathbf{x}_{s,i}) \tag{65}$$

where the face value $u^{n+1/2}_{s,i}$ is constructed from the cell center values $u^{n+1/2}_j$ in the neighborhood of cell i using the TVD limiter (62).

5. Numerical tests

We perform a few simple tests to demonstrate the usefulness of the TOTV concept, to confirm that the upwind scheme is truly TOTVD, and to evaluate the evolution of TOTV for the usual second order TVD scheme.

5.1. 2D linear advection equation

We solve the scalar conservation law

$$\frac{\partial u}{\partial t} + \nabla \cdot \mathbf{f}(u, x, y) = 0 \tag{66}$$

on a 2D periodic square domain $-5 \leq x, y \leq 5$ with a flux function

$$\mathbf{f}(u, x, y) = u\mathbf{v}(x, y) \tag{67}$$

The velocity vector field $\mathbf{v}$ depends on the location:

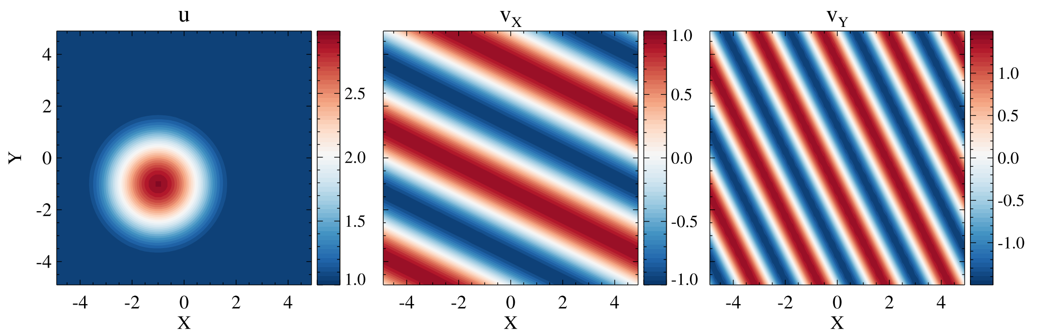

Fig. 5. Initial condition far the test solving a scalar conservation law in 2D. The left panel shows the initial distribution of u, while the other two panels show the two components of the fixed but non-uniform velocity field.

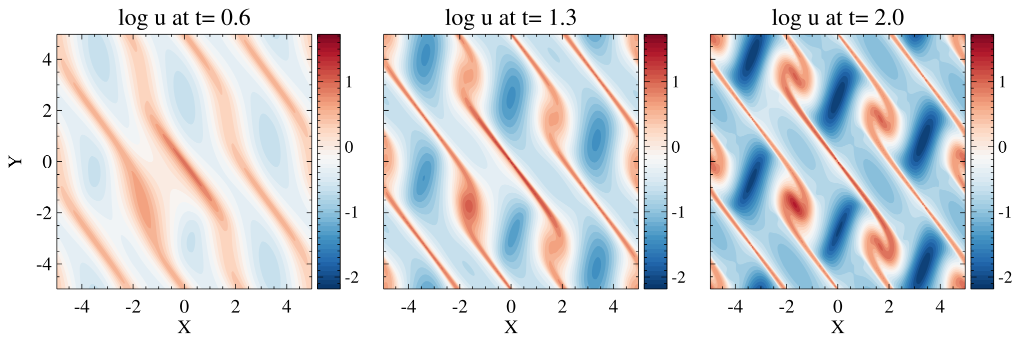

Fig. 6. Time evolution of the 2D linear advection test obtained by the TVD scheme with the MC limiter on a 200×200 grid.

$$
\begin{aligned}
v_x &= -\sin\frac{2\pi(x+2y)}{10} \\
v_y &= -\frac{3}{2}\sin\frac{2\pi(2x+y)}{5}
\end{aligned}
\tag{68}
$$

Note that $\mathbf{v}$ and its derivatives are continuous but it has non-zero divergence. The initial condition is a circular bump centered around the $x = y = -1$ location:

$$
u(t=0) = 1 + 2\cos^2\frac{\pi r}{6} \qquad \text{where} \quad r = \sqrt{(x+1)^2 + (y+1)^2} \tag{69}
$$

for $r \le 3$ and $u(t=0) = 1$ otherwise. The initial condition and its first derivatives are continuous. Fig. 5 shows the smooth initial condition and the velocity field.

Fig. 6 shows the time evolution of the solution with the TVD scheme on a 200×200 grid. The time step is fixed to $\Delta t = 1/160$, so it takes 320 time steps to reach the final time $t = 2$. Note that the 10-based logarithm of u is shown, so u varies almost 4 orders of magnitude by time $t = 2$ due to the non-zero divergence of the velocity field. The fast growth of extrema result in a rapidly growing total variation (TV) defined in 2D with the L1 norm as

$$
T^n_{xy} = \sum_i \left(|u^n_{i+1} - u^n_i| + |u^n_{i+N} - u^n_i|\right) \tag{70}
$$

as shown in the top panel of Fig. 7. Clearly, the TVD principle cannot be applied for this equation. In contrast, the TOTV defined by (27) is decreasing as expected from the analytic TOTVD property. The decrease is monotonic for the first order upwind scheme as proven in the previous section. The second order TVD scheme with the minmod limiter also reduces TOTV monotonically (for this particular test), while the sharper MC limiter is almost always (315 times out of 320 time steps, to be exact) TOTVD.

5.2. 2D Burgers equation

We solve the same problem as in the previous subsection, except that the flux function is defined as

$$
\mathbf{f}(u, x, y) = \frac{1}{2}u^2\mathbf{v}(x, y) \tag{71}
$$

The true "velocity" $\partial\mathbf{f}/\partial u = u\mathbf{v}$ is a function of u, which can form discontinuous solutions ("shocks") in a finite time even for an initially smooth solution. In addition, the CFL condition also depends on u, so the time step is adapted according to (56) with $C = 0.9$. If the initial u is positive everywhere, it should remain positive.

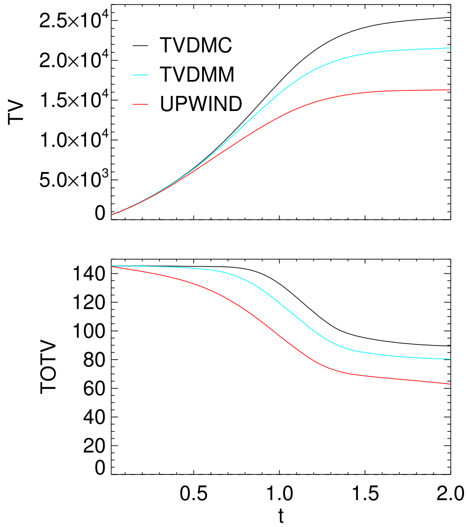

Fig. 7. Time evolution of TV (70), and TOTV (27) while solving the 2D linear advection test with the first order upwind scheme (red), and the second order TVD scheme using the MC (black) and minmod (blue) limiters, respectively, on a 200×200 grid.

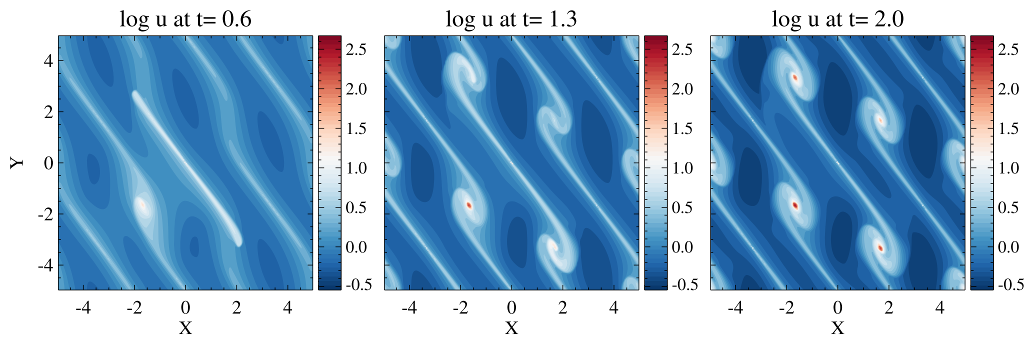

Fig. 8. Time evolution of the 2D Burgers equation test obtained by the TVD scheme with the MC limiter on a 200×200 grid.

Fig. 8 shows the time evolution of u. The maxima are larger and sharper compared to the linear case, on the other hand the minima are less pronounced. There is a discontinuity in the middle of the domain already at $t = 0.6$ due to the divergence of the field and non-linearity of the flux function.

Fig. 9 shows the time evolution of TV and TOTV for the first order upwind and second order TVD schemes. Clearly, the classical TV is growing rapidly, so it cannot be used to characterize the stability of the numerical scheme. For the first order scheme TOTV diminishes monotonically as expected. Finally, for the second order TVD scheme TV is increasing rapidly, but TOTV is decreasing overall, although it is not perfectly monotonic. This suggests that the TOTVD property is applicable to this 2D non-linear equation and it can prove stability for the first order upwind scheme, and it is well-behaved for the second order TVD scheme, although the decrease is not perfectly monotonic (TOTV increases 101 times out of the 1112 time steps for the MC limiter and 20 times out of the 884 times steps for the minmod limiter).

6. Conclusions

We have introduced a new concept, the Total of Time Variation (TOTV) to characterize conservation laws and numerical schemes. We showed that the solutions of nonlinear scalar conservation laws with spatially dependent flux functions satisfy the TOTV diminishing (TOTVD) property analytically, but not the TVD property. Conversely, scalar conservation laws with purely time dependent fluxes satisfy the TVD property, but not TOTVD. Despite this space-time symmetry, purely spatially dependent flux functions are more interesting in practice than purely time dependent flux functions, simply because there are multiple spatial dimensions, but only one temporal dimension. This makes TOTVD interesting and useful in practical applications as demonstrated in [2]. We showed that a numerical scheme satisfying the TOTVD property is stable against non-linearly (or exponentially) growing numerical instabilities.

We proved that the first order upwind scheme is TOTVD for a time step satisfying the usual CFL condition. Our proof requires that the first order scheme is applied at the boundaries between temporally increasing and decreasing subdomains. Anywhere else, any second or higher order scheme can be used. One possible way to construct a second order TOTVD scheme could be based on the Multi-dimensional Optimal Order Detection (MOOD) algorithm [5]. The difficulty is to construct a MOOD-TOTVD scheme

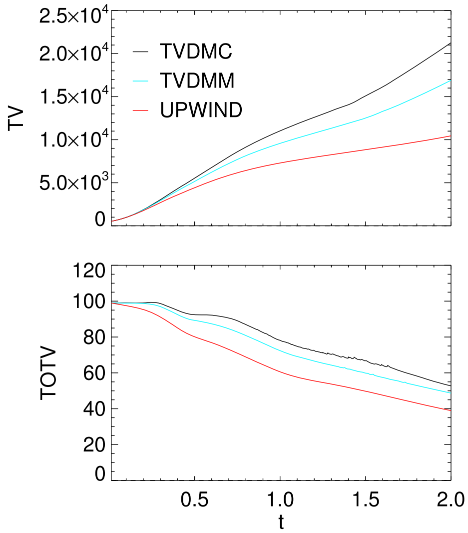

Fig. 9. Time evolution of TV (70), and TOTV (27) while solving the 2D Burgers equation test with the first order upwind scheme (red), and the second order TVD scheme using the MC (black) and minmod (blue) limiters, respectively, on a 200×200 grid.

that does not apply the first order scheme on an unnecessarily large fraction of the computational domain. On the other hand, our numerical tests show that the second order TVD-based scheme (using TVD limiters in each dimension independently) performs well, and it overall reduces TOTV, even if not monotonically. It may be possible to prove that this is a general property of second order TVD-based schemes, which would extend the theoretical understanding of the applicability of these schemes.

Generalization of the TOTVD principle to systems of equations and construction of second order TOTVD numerical schemes remain open questions that can be explored in the future.

CRediT authorship contribution statement

Gabor Toth: Conceptualization, Investigation, Methodology, Software, Visualization, Writing – original draft, Writing – review & editing.

Declaration of competing interest

The authors declare that they have no known competing financial interests or personal relationships that could have appeared to influence the work reported in this paper.

Data availability

Data will be made available on request.

Acknowledgement

The author acknowledges support by the National Science Foundation grant PHY-2027555. The author also thanks Dr. Yuxi Chen and the two reviewers for carefully reading the manuscript and providing useful comments.

References

[1] A. Harten, High resolution schemes for hyperbolic conservation laws, J. Comput. Phys. 49 (1983) 357–393, https://doi.org/10.1016/0021-9991(83)90136-5.
[2] I.V. Sokolov, H. Sun, G. Toth, Z. Huang, V. Tenishev, L. Zhao, J. Kota, O. Cohen, T. Gombosi, High resolution finite volume method for kinetic equations with Poisson brackets, J. Comput. Phys. (2023) 111923, https://doi.org/10.1016/j.jcp.2023.111923.
[3] E. Godlewski, P. Raviart, Hyperbolic Systems of Conservation Laws, Ellipses-Edition Marketing, Paris, France, 1991.
[4] J.B. Goodman, R.J. LeVeque, On the accuracy of stable schemes for 2d scalar conservation laws, Math. Comput. 45 (1985) 15, https://doi.org/10.2307/2008046.
[5] S. Clain, S. Diot, R. Loubère, A high-order finite volume method for systems of conservation laws—multi-dimensional optimal order detection (mood), J. Comput. Phys. 230 (2011) 4028, https://doi.org/10.1016/j.jcp.2011.02.026.